ACERP: Vol. 6, No. 3, (Summer 2020) 55-62

Advanced Ceramics Progress

Research Article

Journal Homepage: www.acerp.ir

Investigation of Microstructure, Hardness, and Corrosion Resistance of Ni-P-GO Electroless Nanocomposite Coating on AZ31D Alloy Surface

M. Hanachi [a], Z. S. Seyedraoufi [a] *, V. Abouei [a]

[a] *Department of Metallurgy and Materials Engineering, Karaj Branch, Islamic Azad University, Karaj, Alborz, Iran*

PAPER INFO

Paper History:

Received 31 May 2020
Accepted in revised form 26 July 2020

Keywords:

Electroless
Phosphorus Content
Ni-P-GO Nanocomposite Coating
Cauliflower
Corrosion

ABSTRACT

In the present study, the Ni-P-GO nanocomposite coating was applied to the surface of AZ31D alloy through electroless plating process. To achieve the nanocomposite coating, 5 g/L Graphene Oxide (GO) was added to the plating bath. By changing the pH of the bath, coatings were created in three ranges of low, medium, and high phosphorus on the surface of AZ31D. According to the results, by increasing the phosphorus content, the amount of graphene oxide absorbed in the coating increased. Microstructural examination by Scanning Electron Microscopy (SEM) showed that all coatings formed on the substrate had the cauliflower morphology. Phase analsis of the coating by X-Ray Diffraction (XRD) showed that at a low phosphorus level, the coating is semi-amorphous; however, with increasing phosphorus content, the coating becomes completely crystalline. The highest hardness value of the specimen was observed with the lowest amount of phosphorus. The microhardness measurments showed that the hardness decreased with increasing the amount of phosphorus so that the minimum hardness of the specimen containing 14.97 wt.% phosphorus was measured at 521 H_{v50}. Contrary to the morphology, phosphorus levels have a significant effect on the structure and hardness of Ni-P-GO nanocomposite coatings. As the amount of phosphorus increased, the corrosion resistance of the coating increased. This is attributed to the reduction of the current of corrosion and more positive potential values.

1. INTRODUCTION

Weight reduction has always been the concern of industry. That is the reason why every year more and more researchers, designers, and craftsmen are turning to use lighter materials. Magnesium and its alloys are among the materials that are widely used to meet the needs of the aerospace, automotive, military, and medical industries due to their low weight. The high strength-to-weight ratio and low density are the main reasons for the importance of magnesium alloys. Poor resistance to abrasion and corrosion is the Achilles's heel of magnesium alloys. Therefore, these shortcomings have challenged the frequent use of this material [1-4].

Every year, various methods such as thermal spraying, veneering, work surface friction, surface processing, and composite fabrication by turbulent friction process, sol-gel, and electroless and electrical plating are used to improve the surface properties of magnesium alloys [5-10]. Electroless plating is usually considered as the first option due to the low cost of the process, the uniform layer created, and the abrasion and corrosion resistance of the formed layer.

Electroless coatings usually based on nickel, copper, cobalt, silver, and serum are formed on the surface of the part according to the user's needs. Nickel-based coatings are divided into three types according to the type of bath and the composition of the layer created: nickel, nickel-boron, and nickel-phosphorus electroless coatings [11]. To improve the properties of these coatings, they are usually either alloyed with Mo, Co, Cr, and Cu elements, or form composite through secondary phases [12]. These two approaches both in amorphous and crystalline states lead to increased hardness and wear resistance of the coating.

Due to the short duration of the electroless process, these coatings are formed in the amorphous state. Through heat treatment, the amorphous structure becomes crystalline and the energy for the formation of intermediate phases (nickel-phosphorus intermetallic compounds) is supplied [13]. Crystallization and distribution of intermediate phases increase the hardness and wear resistance of the coating [13]. Recent research has shown that the addition

* Corresponding Author Email: z.seyedraoufi@kiau.ac.ir (Z. S. Seyedraoufi)
https://doi.org/10.30501/acp.2020.233518.1038

of graphene oxide nanoparticles increases wear resistance by reducing the coefficient of friction, which is increased by heat treatment at 400°C [14,15].
However, previous researchers have expressed opposing views on either adverse effects or positive effects of heat treatment on the corrosion resistance of nickel-phosphorus coatings.
In the present study, Ni-P-GO composite electroless coatings with different amounts of phosphorus were formed on AZ31D alloy surface. The aim of this study was to achieve the optimal amount of phosphorus to achieve the highest values of hardness and corrosion resistance by formation of composite coating with graphene oxide (GO) nanoplates.
Electroless plating coatings in acidic baths are difficult to form on a magnesium substrate. Therefore, this research is one of the few researches carried out to create electroless nanocomposite coating on magnesium substrate.

2. MATERIALS AND METHODS

In this study, the AZ31D magnesium-based alloy plate purchased from Iraninan company of NOVIN RAHYAFT with dimensions of 20 × 20 × 5 mm was used as a substrate. The chemical composition of the alloy is shown in Table 1. GO was used to fabricate Nickel-phosphorus composite coating. GO was purchased from Indian company of UNITED NANOTECH INNOVATIONS. Specifications of graphene oxide nanoplates are presented in Table 2.

TABLE 1. The chemical composition of the substrate obtained from quantometry

El.	Mg	Al	Zn	Mn	Sn	Fe	Ni
wt.%	Base	3.38	1.19	0.44	0.01	0.005	0.005

TABLE 2. Specifications of graphene oxide nanoplates

Lateral Dimensions (μm)	Density (g/cc)	Surface Space (BET) (m^2/g)	Layers number	Purity (%)	Thickness (nm)
5-10	0.42	Less than 120	8-10	99.999	3-6

Specimens were polished by SiC abrasive papers up to No. 1200. Polished specimens were washed with acetone and then, with distilled water. After washing, the specimens were air-dried to obtain a clean surface with suitable surface roughness. Finally, the following steps were performed to activate the specimens in accordance with ASTM B480 standard:
a) Primary cleaning with detergent and water.
b) Degreasing with acetone in an ultrasonic bath for 20 minutes.
c) Chromate conversion coating in 25% chromic acid with 11% nitric acid for 40 seconds.
d) Removal of surface oxide films in a mixture of 5.5% fluoride acid (HF) for 10 minutes.
After each step, the specimens were washed in distilled water and in the final step, they were immediately immersed in an electroless bath. To make composite coating, 5 g/L GO was added to the plating bath. In order to facilitate the plating process, some part of the specimens (substrate) was drilled so that it could be easily placed in the bath. The chemical composition of the bath used in this study is shown in Table 3.

TABLE 3. Composition of plating bath for Ni-P coating on AZ31D alloy surface

Chemical Compounds	$NiSO_4.6H_2O$ (g/L)	$NaH_2PO_2.H_2O$ (g/L)	CH_3COONa (g/L)	Lactic acid (ml/L)
Concentration	30	25	25	20

The plating process was performed in the temperature range of 85 to 90˚C. Due to the oxidation of magnesium specimens during the electroless process, 0.6% HF was added to the solution before starting the coating process. This solution was placed in an ultrasonic bath for 1 hour to obtain a suitable dispersion of GO particles in the solution.
Ni-P coating was formed in baths with acidic conditions, and the hardness of this coating was completely affected by pH variations; therefore, pH control of these solutions is very important [11]. As the precipitate forms, the pH of the solution changes over time, regularly controlled by adding dilute NaOH. Due to the high potential of the substrate, applying Ni-P coating to the AZ31D alloy requires a catalyst to initiate the chemical reaction. A small iron nail was used as the reaction catalyst. The catalyst was placed in the plating bath for 20 seconds at the specified temperature and pH. After the electroless solution reached the desired temperature and pH, a magnetic stirrer system at 350 rpm was used to prevent the particles from settling in the bath during the plating process. The electroless process was performed for one hour. In this study, Ni-P electroless coatings with three phosphorus percentages of P< 6%, P = 6-10%, and P>10% were used and pH values were fixed at 3.5, 4.5, and 5.5 during the formation of electroless Ni-P coating.
Microstructural features of the coated specimens were analyzed. The X-ray diffraction pattern was obtained by the Dutch Philips X-pert device using a Cu kα lamp with a wavelength of $\lambda = 1.542$ Å at an angle of 20 to 80 degrees with step size = 0.02. The resulting patterns were analyzed by Xpert software to identify each of the possible phases.

To investigate the microstructure, a scanning electron microscope manufactured by the Czech company TESCAN model VEGA TS5130MM with a working voltage of 20.00 kV was used. Secondary electron mode was used for imaging. In addition, the device was equipped with elemental analysis using X-ray EDS, which was used for the elemental exploration of the coating surface or any specific point of the coating.
Corrosion resistance of all specimens including substrate, plated, and heat treated specimens was investigated. The corrosion test was performed by the EG & G 263A Potentiostat/Galvanostat Instrument in the environment and with Saturated Calomel reference Electrode (SCE). Platinum used as an auxiliary electrode and the coated steel substrate as a working electrode were placed in NaCl solution with 3.5% concentration. In this test, the desired parts were exposed to corrosive environment (coated parts) and the rest of the surface of the specimens was covered with varnish. The scanning speed of potential of 1 mV/s in the range of ±400 mv around the open circuit potential was considered in polarization tests. Prior to measurement, the specimens were placed in corrosive environment for one hour to establish the potential of the open circuit.

3. RESULTS AND DISCUSSION

Fig. 1 shows the SEM morphological images of nickel-phosphorus-oxide graphene coatings with different amounts of phosphorus. What is clear in all three parts of Fig. 1 is the formation of the nanocomposite coating with the morphology of the cauliflower. This type of coating is common to all electroless coatings [16]. Due to the presence of porosity between the colonies, this structure has self-lubrication properties and shows good abrasion resistance [11, 13]. The size of colonies is affected by process parameters [17].
Given that all process variables have been constant, this change in colony size can be considered as a function of phosphorus content. As shown in Fig. 2, increasing the amount of phosphorus has led to a decrease in the size of colonies, which can be attributed to an increase in the nucleation sites in the coating and a decrease in the crystallite sizes. Each colony is made up of millions of crystallites [17].

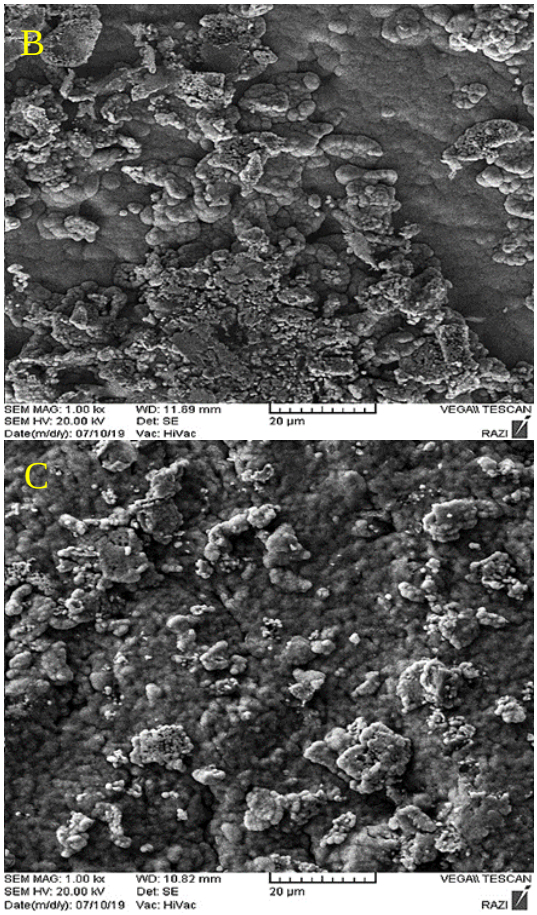

Figure 1. SEM images of nickel-phosphorus-graphene oxide nanocomposite coatings (A) less than 6% phosphorus (B) 6 to 10% phosphorus (C) more than 10% phosphorus

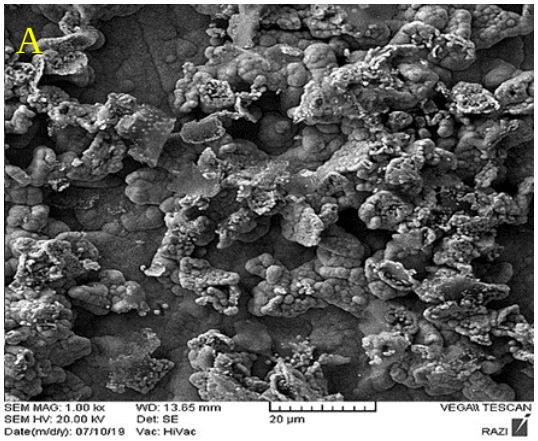

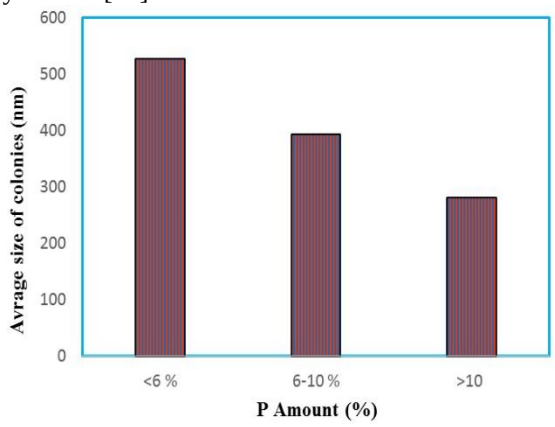

Figure 2. The relation between the amount of phosphorus in the nickel-phosphorus-graphene oxide nanocomposite coatings and coating colonies

Table 4 shows the local analysis results of the area marked with a yellow square in Figure 1. It should be noted that as shown in Table 4, the amount of graphene oxide absorbed in the coating has increased with increasing phosphorus content. Increasing the amount of carbon and oxygen in the EDS results confirms this fact. The reason for this is the greater tendency of phosphorus than nickel to react with carbon.

TABLE 4. EDS results of Ni-P-GO nanocomposite coatings

Specimens	Amount of Elements		
	Element	Wt. %	At. %
P < 0.6%	Ni	80.15	64.85
	P	5.21	12.14
	C	1.98	4.07
	O	12.66	19.21
6-10 % P	Ni	73.12	50.21
	P	7.66	15.91
	C	2.31	7.17
	O	16.91	26.71
P > 10%	Ni	61.72	41.41
	P	14.97	18.18
	C	4.04	13.30
	O	19.27	27.11

Fig. 3 shows the SEM images of the cross-sectional area of the coatings. All coatings are uniformly formed on the substrate surface. One of the characteristics of electroless coatings is their uniformity. Due to the lack of external flow during the application of these coatings, there is no accumulation of flow in sharp points or no uniformity in some parts of the coating [18]. It seems that during the process and nucleation of the first points in the coating, a reaction has taken place between the magnesium substrate and the nickel-based coating which concludes in the formation of a very thin intermetallic layer (Mg_2Ni). The formation of an intermetallic compound between nickel and magnesium does not require high energy and temperature according to the literature [19]. As the coating forms and the amount of magnesium in the substrate decreases, the coating becomes rich in nickel and the formation of the coating returns to its normal state.

In Figure 4, elemental mapping image of Ni, P, and C in the medium phosphorus coating is shown. As can be seen, the carbon element that characterizes graphene oxide is well distributed in different parts of the coating. On the other hand, Figure 4 shows that phosphorus is also well distributed in a nickel matrix.

Fig. 5 shows the XRD patterns of all three coatings. As shown, at the highest phosphorus level, the coating is formed in the crystalline state with a small amount of amorphous phase on the substrate surface. The intermetallic compound created on the substrate discussed in the previous section is well illustrated in the XRD results. Fig. 5 shows also the XRD pattern of the specimen with moderate phosphorus. In this image, it is clear that the amorphous phase located at 45 degrees has reached a minimum.

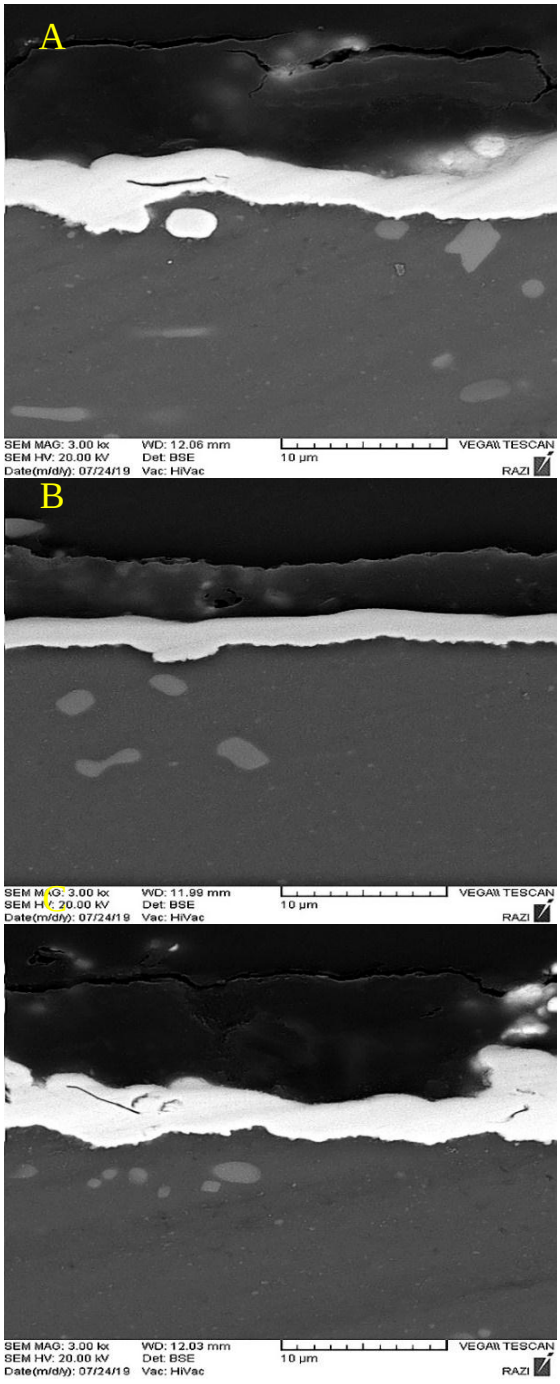

Figure 3. Cross-sectional SEM images of nickel-phosphorus-graphene oxide nanocomposite coatings (A) less than 6% phosphorus (B) 6 to 10% phosphorus (C) more than 10% phosphorus

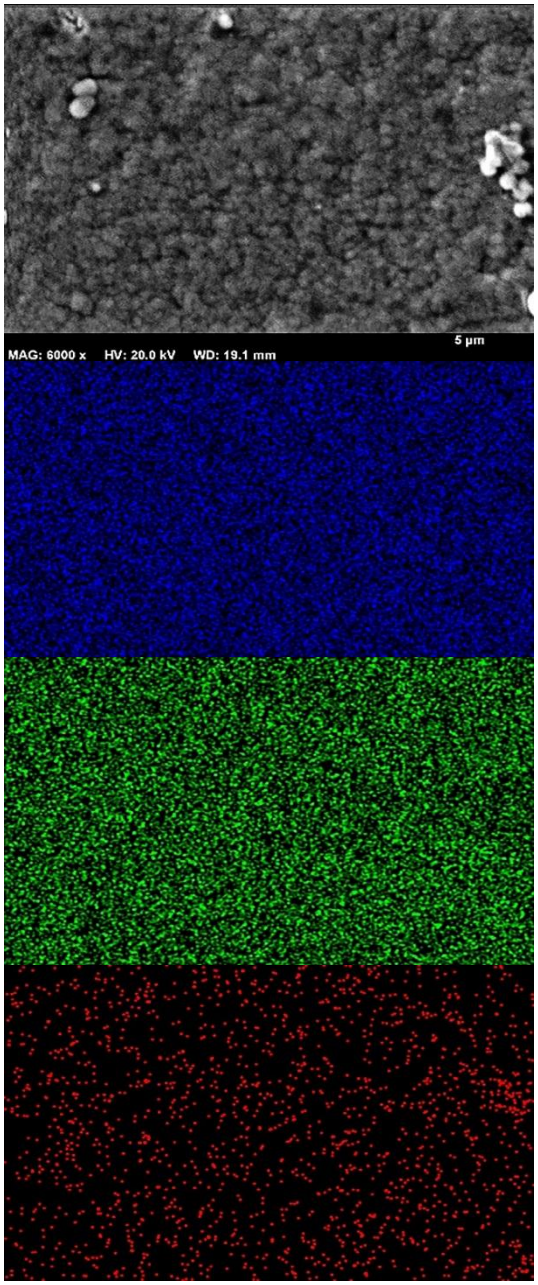

Figure 4. Elemental mapping images of Ni(blue), P(green), and C(red) in the medium phosphorus coating

As the pH of the bath decreases, the amount of phosphorus in the coating decreases. As shown in the XRD pattern images, the crystallinity has also intensified with lowering the phosphorus content. It is stated in the literature that increasing the amount of phosphorus or boron increases the possibility of amorphous coating due to rise in segregation of alloying elements [20]. It is also observed that the amount of nickel-phosphorus intermetallic compound (Ni_2P) has increased for higher phosphorus content.

As shown in Table 4, with increasing phosphorus content, the amount of graphene oxide absorbed in the coating has increased. Increasing the amount of carbon and oxygen in the EDS results confirms this.

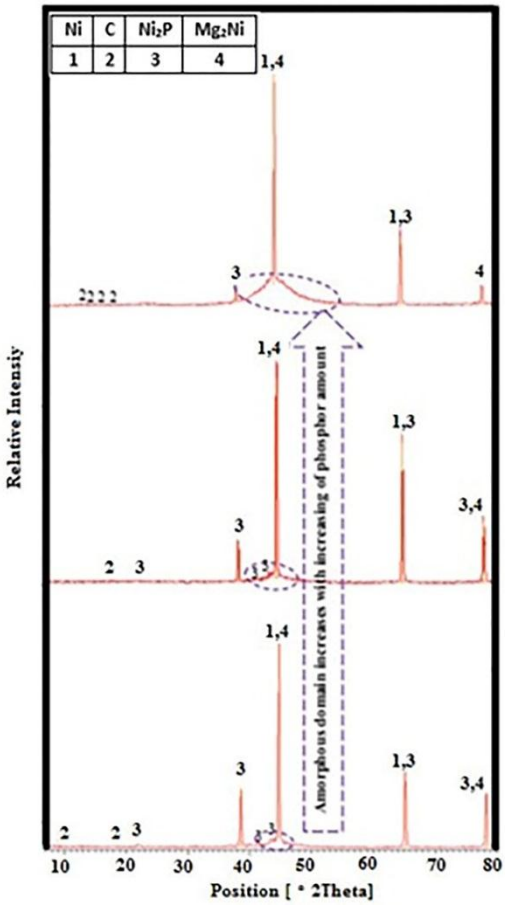

Figure 5. XRD pattern of nickel-phosphorus-graphene oxide nanocomposite coatings

Thickness, crstallite size, and lattice strain values of the specimens with different P contents are given in Table 5. As indicated, the higher values of pH has expanded the thickness of the coating. Previous researches have also stated that increasing the pH in the acidic range results in an increase in the thickness of the coating, and when the pH reaches the neutral point, the thickness of the coating starts to reduce. The thickness of the coating in the basic range reaches its lowest level [21]. The general reaction of nickel ion reduction by hypophosphite can be considered as relation (1).

TABLE 5. Thickness, cystallite size, and lattice strain of Ni-P-GO nanocomposite coatings

Specimens	Low (P)	Medium (P)	High (P)
Thickness (µm)	1.24	2.19	3.01
Crystallite size (nm)	41	37	25
lattice strain	2186.636363	2358.723558	3490.909090

$$3Na_2PO_2 + 3H_2O + NiSO_4 \rightarrow 3NaH_2PO_3 + H_2SO_4 + 2H_2 + Ni \quad (1)$$

The above reaction can also be formulated as in Relation (2):

$$2H_2PO_2^- + Ni^{++} + 2H_2O \rightarrow 2H_2PO_3^- + H_2 + 2H^+ + Ni \quad (2)$$

Moreover, some changes are made as seen in Relation (3):

$$Ni^{++} + H_2PO_2^- + H_2O \rightarrow Ni + H_2PO_3 + 2H^+ \quad (3)$$

All of these reactions take place on the catalytically active surface by applying external energy, i.e. heating the solution to a temperature between 60 and 95˚C. In addition to the formation of metallic nickel, some molecular hydrogen is also produced, which is removed during heat treatment [22]. Apart from these changes, the formation of H^+ ions leads to further acidification of the bath, while orthophosphate ($H_2PO_3^-$) ions will also form. The nature of the partial reactions involved during precipitation of nickel ions in solution by reduction with the use of sodium hypophosphite has not yet been fully understood. According to studies, partial reactions of the process are given in Relations (4 to 9) [22].

$$H_2PO_2^- + H_2O \rightarrow H^+ + HPO_3^- + 2H_{ads} \quad (4)$$

$$Ni^{++} + 2H_{ads} \rightarrow Ni + 2H^+ \quad (5)$$

$$2H_{ads} \rightarrow H_2 \quad (6)$$

$$H_2PO_2^- + H_2O \rightarrow H_2PO_3^- + H_2 \quad (7)$$

$$H_2PO_2^- + H_{ads} \rightarrow H_2O + OH^- + P \quad (8)$$

$$3H_2PO_2^- \rightarrow H_2PO_3^- + 2OH^- + 2P + H_2O \quad (9)$$

All of the above steps occur during reduction reactions simultaneously. The rate of these reactions depends on various factors in the bath such as pH, temperature, and chemical composition. From Relations (8) and (9), it can be concluded that in addition to nickel, the phosphorus element is also formed in the coating. In general, Reaction 8 is slower than Reaction 3. If the pH decreases, reactions (8) and (9) tend to proceed towards the formation of more phosphorus in the coating while Reactions (5) and (3) tend to proceed towards nickel decrease.

Therefore, a decrease in pH leads to a decrease in the rate of Ni-P deposition, while the amount of phosphorus in the coating also increases.

Fig. 6 demonstrates the hardness changes of the specimens with increasing the phosphorus content. Composite coating formation increases the hardness of the coating due to creation of obstacles to the movement of dislocations. Therefore, the hardness of composite coatings is naturally higher than that of non-composite coatings.

Increasing the amount of phosphorus has resulted in a decrease in hardness. At first glance, the increase in phosphorus levels due to the increase in precipitates should have led to an increase in hardness. However, with increasing phosphorus levels, the hardness in this study has decreased.

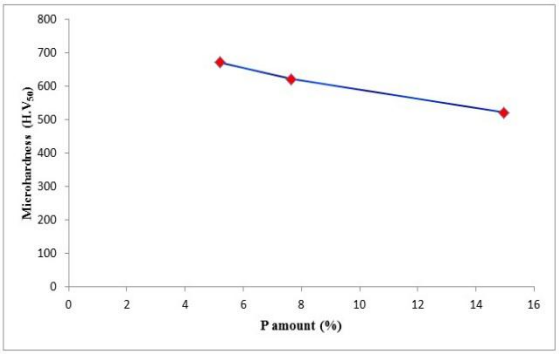

Figure 6. Variations of hardness in terms of coating P content

As shown in Table 5, with increasing phosphorus content, the nucleation of Ni_2P compounds within crystalllites leads to an increase in lattice strain and, consequently, an decrease in the size of the crystallites, which in turn increases the crystallization of the coating due to compressive residual stress. The growth of new nuclei within the grains has led to an increase in size, which has resulted in a reduction in hardness. In Fig. 7, polarization corrosion diagram of all specimens is represented.

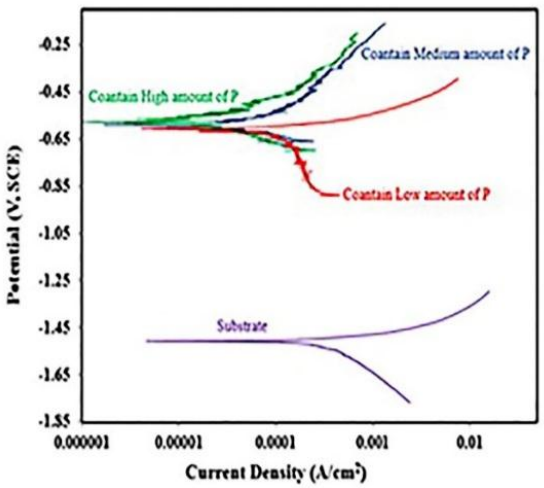

Figure 7. Polarization curves of the specimes containing different phosphorous content

The information extracted from Fig. 7 is presented in Table 6. As it is obvious, with increasing the amount of phosphorus, i_{corr} has decreased and the potential has shifted to the positive values. As the amount of phosphorus increases, the density of the phosphorous-rich layer on the surface increases during corrosion which in turn controls the current rate.

TABLE 6. Parameters extracted from polarization curves

Specimens	i_{corr} (A/cm^2)	E_{corr} (V)	Ba (V/Dec.)	Bc (V/Dec.)	Rp (Ω.cm^2)
Substrate	29.00E-05	-1.51	0.060	0.22	70.59
Low (P)	12.00E-05	-0.62	0.087	0.056	314.81
Medium (P)	2.90E-05	-0.59	0.117	0.074	678.72
High (P)	1.74E-05	-0.56	0.111	0.118	1689.50

The literature reports on Ni–P coatings indicate that preferential dissolution of nickel occurs at open circuit potential, leading to the enrichment of phosphorus on the surface layer. The enriched phosphorus surface reacts with water to form a layer of adsorbed hypophosphite anions ($H_2PO_2^-$). This layer in turn will block the water supply to the metal surface, thereby preventing the hydration of nickel, which is considered to be the first step to form either soluble Ni^{2+} species or a nickel passive film [23-25]. On the other hand, as shown in the previous sections, the absorption of graphene oxide increases with increasing the amount of phosphorus in the composite coating, which is also effective in reducing the corrosion rate.

Immediately after immersion of the coating inside the corrosive solution, nickel begins to dissolve, resulting in increased current density. After a short time, the current begins to decrease to reach a stable level due to the formation of a passive layer on the surface. Elsener et al. reported that by placing the coating in chloride corrosive environments, the dissolution rate of nickel would be higher than that of phosphorus. Therefore, a two-layer passive film consisting of a phosphate layer and a phosphorous-rich layer forms on the surface. [23]. The presence of the passive phosphate layer on the raw coatings and oxide layer on the heat-treated coatings are the reasons for achieving good corrosion resistance of these coatings [24].

The presence of the passive region is observed for all specimens in the polarization curves. It can be seen that the lowest density of passive current and the greatest range of passive potential are related to the coating with the highest phosphorus content. Specimens coated with the medium phosphorus and high phosphorus contents have the highest corrosion resistance, lowest current density, and maximum corrosion potential of all other specimens and the substrate without any coating exhibits the lowest corrosion resistance among the other specimens. This indicates that in any case, the coating improves corrosion resistance.

In general, all nickel-phosphorus electroless coatings exhibit good corrosion resistance [22]. The reason for this is related to the presence of phosphorus atoms in the coating structure. In fact, by placing the specimens in the corrosive environment and dissolving nickel, the surface is enriched with phosphorus atoms, which in response to the water molecules form an absorbent layer of hypophosphite anions. This layer acts as a protective barrier, preventing water molecules to reach the surface of the coating, hydrating the nickel, and further dissolving it [25, 26].

This research can help researchers achieve high hardness and corrosion resistance in nanocomposite coatings before heat treatment and is effective in selecting the optimal parameters for the application of electroless nanoomposite coatings on magnesium alloys.

4. CONCLUSIONS

From the present study, it can be concluded that:

1) As the amount of phosphorus in the coating increases, the size of the colonies in the coating with the morphology of the cauliflower decreases.
2) With increasing the phosphorus in the coating, the absorption rate of graphene oxide nanoplates increases.
3) Increasing the amount of phosphorous in the coating, increases the crystallinity of the coating and the intermediate phase of Ni2P.
4) With invreasing the amount of phosphorus, the thickness of the coating increased from 1.24 to 3.01 µm.
5) As the amount of phosphorus in the coating increases, the hardness of the coating decreases. the minimum hardness in the specimen containing 14.97 wt.% phosphorus was measured 521 H_{v50}.
6) With increasing the amount of phosphorus in the coating, the corrosion resistance of the coating increases. The lowest current density (1.74E-05 A/cm^2) and the highest corrosion resistance (1689.50 Ω.cm^2) were obtained in the sample containing the highest phosphorus.

5. ACKNOWLEDGMENTS

The authors would like to thank you the staffs of ceramic shaping laboratory of materials and energy research center, specially Y. Shajari and E. Jabari, for their technical supports.

REFERENCES

1. Gu, C., Jiang, Z., "Multilayer Ni-P Coating for Improving the Corrosion Resistance of AZ91D Magnesium Alloy", ***Advanced***

Engineering Materials, Vol. 7, No. 11, (2005), 1032-1036. https://doi.org/10.1002/adem.200500136

2. Kanta, A. F., Vitry, V., Delaunois, F., "Wear and corrosion resistance behaviours of autocatalytic electroless plating", ***Journal of Alloys and Compounds***, Vol. 486, No. 1-2, (2009), L21-L23 . https://doi.org/10.1016/j.jallcom.2009.07.038

3. Hu, R., Su, Y., Liu, Y., Liu, H., Chen, Y., Cao, C., Ni, H., "Deposition Process and Properties of Electroless Ni-P-Al_2O_3 Composite Coatings on Magnesium Alloy", ***Nanoscale Research Letters***, Vol. 13, No. 1, (2018), 1-8. https://doi.org/10.1186/s11671-018-2608-0

4. Ashtiani, A. A., Faraji, S., Iranagh, S. A., Faraji, A. H., "The study of electroless Ni–P alloys with different complexing agents on Ck45 steel substrate", ***Arabian Journal of Chemistry***, Vol. 10, (2017), S1541-S1545. https://doi.org/10.1016/j.arabjc.2013.05.015

5. Thirumalaikumarasamy, D., Shanmugam, K., Balasubramanian, V., "Corrosion performance of atmospheric plasma sprayed alumina coatings on AZ31B magnesium alloy under immersion environment", ***Journal of Asian Ceramic***, Vol. 2, No. 4, (2014), 403-415. https://doi.org/10.1016/j.jascer.2014.08.006

6. Rao, K. P., Sankar, A., Rafi, H. K., Ram, G. J., Reddy, G. M., "Friction surfacing on nonferrous substrates: a feasibility study", ***The International Journal of Advanced Manufacturing Technology***, Vol. 65, No. 5-8, (2013), 755-762. https://doi.org/10.1007/s00170-012-4214-0

7. Liu, Q., Ma, Q. X., Chen, G. Q., Cao, X., Zhang, S., Pan, J. L., Zhang, G., Shi, Q. Y., "Enhanced corrosion resistance of AZ91 magnesium alloy through refinement and homogenization of surface microstructure by friction stir processing", ***Corrosion Science***, Vol. 138, (2018), 284-296. https://doi.org/10.1016/j.corsci.2018.04.028

8. Han, H. M., Wang, D. T., Yu, H. Q., Zuo, M., Wang, L. H., Zhao, D. G., "Ceria Coatings Prepared by Sol-Gel Approach on AZ91 Magnesium Alloy", In ***Materials Science Forum***, Vol. 898, (2017), 1369-1380, Trans Tech Publications Ltd. https://doi.org/10.4028/www.scientific.net/msf.898.1369

9. Zhang, J., Song, Z., Yu, G., Hu, B., Zhang, X., "Corrosion Behavior of Electroless Ni-P/Ni-B Coating on Magnesium Alloy AZ91D in NaCl Environment", ***International Journal of Electrochemcal Science,*** Vol. 11, (2016), 10053-10066. https://doi.org/10.20964/2016.12.57

10. Huang, C. A., Yeh, Y. H., Lin, C. K, Hsieh, C. Y., "Copper Electrodeposition on a Magnesium Alloy (AZ80) with a U-Shaped Surface", ***Materials***, Vol. 7, No. 11, (2014), 7366-7378. https://doi.org/10.3390/ma7117366

11. Shajari, Y., Alizadeh, A., Seyedraoufi, Z. S., Razavi, S. H., Shamakhi, H., "The effect of heat treatment on wear characteristics of nanostructure Ni-B coating on marine bronze", ***Materials Research Express***, Vol. 6, No. 10, (2019), 105040. https://doi.org/10.1088/2053-1591/ab395d

12. Serin, I. G., Göksenli, A., Yüksel, B., Yildiz, R. A., "Effect of Annealing Temperature on the Corrosion Resistance of Electroless Ni-B-Mo Coatings", ***Journal of Materials Engineering and Performance***, Vol. 24, No. 8, (2015), 3032-3037. https://doi.org/10.1007/s11665-015-1568-0

13. Shajari, Y., Porhonar, M., Seyedraoufi, Z. S., Razavi, S. H., Baghdadabad, D. M., Yousefnia, H., Farahani, M., "Improvement of the NiBrAl casting alloy surface properties by electroless Ni-B plating for dynamic marine application", ***Physical Mesomechanics***, Vol. 23, No. 1, (2020), 81-88. https://doi.org/10.1134/s1029959920010087

14. Jiang, J., Chen, H., Zhu, L., Qian, W., Han, S., Lin, H., Wu, H., "Effect of heat treatment on structures and mechanical properties of electroless Ni–P–GO composite coatings", ***RCS Advances***, Vol. 6, No. 110, (2016), 109001–109008. https://doi.org/10.1039/c6ra22330c

15. Wu, H., Liu, F., Gong, W., Ye, F., Hao, L., Jiang, J., Han, S., "Preparation of Ni–P–GO composite coatings and its mechanical properties", ***Surface and Coating Technology***, Vol. 272, (2015), 25-32. https://doi.org/10.1016/j.surfcoat.2015.04.028

16. Oraon, B., Majumdar, G., Ghosh, B., "Improving hardness of electroless Ni-B coating using optimized deposition conditions and annealing", ***Materials & Design***, Vol. 29, No. 7, (2008), 1412-1417. https://doi.org/10.1016/j.matdes.2007.09.005

17. Loto, C. A., "Electroless Nickel Plating : A Review", ***Silicon***, Vol. 8, No.2, (2016), 177-186. https://doi.org/10.1007/s12633-015-9367-7

18. Zhang, W. X., Jiang, Z. H., Li, G. Y., Jiang, Q., Lian, J. S., "Electroless Ni-P/Ni-B duplex coatings for improving the hardness and the corrosion resistance of AZ91D magnesium alloy", ***Applied Surface Science***, Vol. 254, No. 16, (2008), 4949–4955. https://doi.org/10.1016/j.apsusc.2008.01.144

19. Portnoi, V. K., Leonov, A. V., Fedotov, S. A., "Solid-phase synthesis in Ni-Mg and Ni-Mg-C systems upon ball milling of powder mixtures", ***Bulletin of the Russian Academy of Sciences: Physics***, Vol. 73, No. 9, (2009), 1211. https://doi.org/10.3103/s1062873809090081

20. Baskaran, I., Kumar, R. S., Narayanan, T. S., Stephen, A., "Formation of electroless Ni–B coatings using low temperature bath and evaluation of their characteristic properties", ***Surface and Coatings Technology***, Vol. 200, (2006), No. 24, 6888–6894. https://doi.org/10.1016/j.surfcoat.2005.10.013

21. Czagány, M., Baumli, P., "Effect of pH on the characterstic of electroless Ni-P coatings", ***Journal of Mining and Metallurgy Section B Metallurgy***, Vol. 53, No. 3, (2017), 327-332. https://doi.org/10.2298/jmmb170530020c

22. Riedel, W., ***Electroless Nickel Plating***, Metals Park, Ohio: ASM International, (1991).

23. Ashassi-Sorkhabi, H., Es'haghi, M., "Corrosion resistance enhancement of electroless Ni–P coating by incorporation of ultrasonically dispersed diamond nanoparticles", ***Corrosion Science***, Vol. 77, (2013), 185-193. https://doi.org/10.1016/j.corsci.2013.07.046

24. Elsener, B., Crobu, M., Scorciapino, M. A., Rossi, A., "Electroless deposited Ni–P alloys: corrosion resistance mechanism", ***Journal of Applied Electrochemistry***, Vol. 38, No. 7, (2008), 1053-1060. https://doi.org/10.1007/s10800-008-9573-8

25. Bozzoni, B., Lenardi, C., Serra, M., Faniglulio, A., "Electrochemical and X-ray photoelectron spectroscopy investigation into anodic behaviour of electroless Ni–9.5 wt%P in acidic chloride environment", ***British Corrosion Journal***, Vol. 37, No. 3, (2002), 173-181. https://doi.org/10.1179/000705902225006589

26. Ghavidel, N., Allahkaram, S. R., Naderi, R., Barzegar, M., Bakhshandeh, H., "Corrosion and wear behavior of an electroless Ni-P/nano-SiC coating on AZ31 Mg alloy obtained through environmentally-friendly conversion coating", ***Surface and Coating Technology***, Vol. 382, (2020), 125156. https://doi.org/10.1016/j.surfcoat.2019.125156